Proceedings of ITC18, 2008

Configuration Control Experiment in Heliotron J

H. Okada, S. Kobayashi, K. Nagasaki, T. Mizuuchi, S. Yamamoto, G. Motojima[a], S. Watanabe[b], K. Mukai[b], S. Mihara[b], Y. Kowada[b], K. Hosaka[b], A. Matsuyama[b], Y. Nakamura[b], K. Hanatani, N. Nishino[c], Y. Nakashima[d], K. Nagaoka[a], T. Mutoh[a], Y. Suzuki[a], M. Yokoyama[a], A.C. Fernández[e], Á,A, Cappa[e], S. Konoshima, K. Kondo[b] and F. Sano.

Institute of Advanced Energy of Kyoto University, Uji 611-0011, Japan

[a] National Institute for Fusion Science,, Toki 509-5292, Japan

[b] Graduate School of Energy Science, Kyoto University, Uji 611-0011, Japan

[c] Graduate School of Engineering, Hiroshima University, Higashi-Hiroshima 739-8527, Japan

[d] Plasma Research Center. University of Tsukuba, Tsukuba 305-8577, Japan

[e]Laboratorio Nacional de Fusión, EURATOM-CIEMAT, Madrid 28040, Spain

Heliotron J is a flexible configuration device to explore a new concept optimization for the helical-axis heliotron configuration. The field ripple along the toroidal direction, which is called 'bumpiness' is a key component for the improvement of the particle confinement. From the fast ions generated by the ICRF minority heating, the high bumpy configuration is most favorable and the fast ions of about 30 keV are observed. The toroidal current control is also important for the Heliotron J field configuration. Using the combination of the change of the bumpiness and the deposition position, the toroidal current can be controlled by about 7 kA. The bumpy field dependence on the global confinement is investigated for ECH and NBI plasmas. The confinement in the high and medium bumpy configurations is better than that in the low bumpy configuration. The difference of the bumpy dependence for the ECH and NBI plasmas is possibly caused by the improved fast-ion confinement for the NBI plasmas in the high bumpy configuration.

Keywords: helical-axis heliotron, bumpiness control, fast ion confinement, non-inductive current, improved confinement

1. Inroduction

The optimization of the field configuration is very important for helical systems since there is large ripple loss in the collisionless regime for simple stellarator/heliotron. There are various advanced concepts proposed for this purpose, for example, quasi-omnigeneity [1], quasi-helical symmetry [2], quasi-axisymmetry [3] and so on. Heliotron J belongs to a quasi-omnigeneous concept among them, and is a low-shear helical-axis heliotron (major radius of the torus R_0 = 1.2 m, minor radius of the plasma a = 0.1-0.2 m, magnetic field on the axis $B_0 \leq$ 1.5 T, helical-coil pole number L = 1, pitch number M = 4) [4, 5, 6]. Using controllable five sets of coil systems, Helitoron J realizes a wide range of configurations by changing the coil-current ratios.

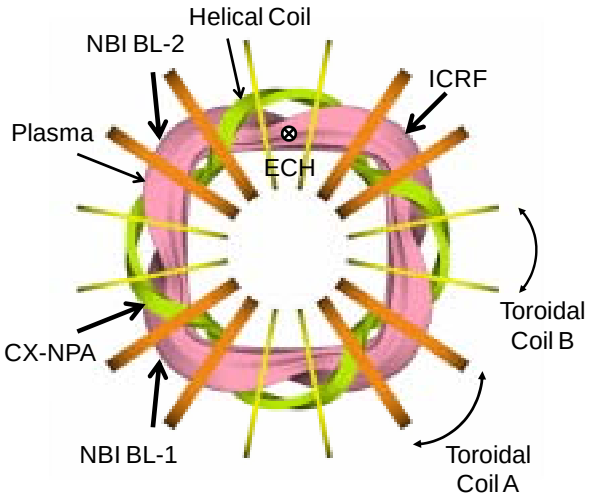

Fig. 1 Top view of Helitoron J. The helical coil and the two types of toroidal coils are illustrated. The positions of the three heating systems (ECH, NBI and ICRF) are also indicated.

The top view of the helical coil and the plasma is shown in Fig. 1. Three heating systems, which are the neutral beam injection (NBI), the ion cyclotron range of frequency (ICRF) and the electron cyclotron (EC) heating devices are installed in Heliotron J. A plasma is generated by using vertically-injected ECH, which is the second harmonic (70 GHz) X-mode and has power of 450 kW. The direction of the toroidal field is clockwise in Fig.1 for the normal operation. The two tangential-injection NB devices are installed; whose injection power and

author's e-mail: okada@iae.kyoto-u.ac.jp

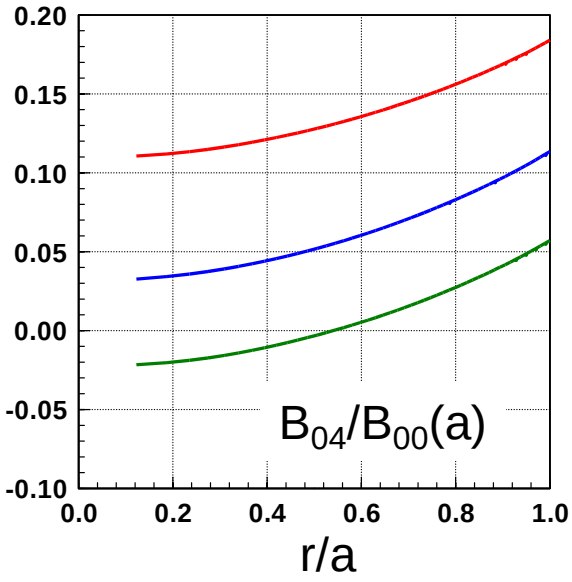

Fig. 2 The profiles of the bumpy ripples for the three bumpy configurations.

acceleration voltage are 700 kW and 30 kV for each unit. Two loop antennas for the ICRF heating are installed on the low field side of the corner section (upper-right corner in Fig. 1). The frequency of the ICRF is 19 - 23.2 MHz and the injection power is 400 kW for each antenna.

In this paper, the results of the control experiments by changing the bumpiness in the field configuration, which is one of the Fourier components in the Boozer coordinates, are described. The bumpy field component is a field ripple along the toroidal direction. This component is generated by the two sets of toroidal coils and the helical coil. If the current ratio of the toroidal coil A to the toroidal coil B (See Fig. 1) is unity, the sign of the bumpy component is equal to that of the helical ripple. Both the value of the bumpiness and the radial profile is effective for the improvement of the particle confinement in this magnetic configuration. The effectiveness of the bumpy component is investigated for (i) high energy ion confinement using ICRF minority heating, (ii) a non-inductive current in ECH plasmas and (iii) energy confinement for ECH or NBI plasmas. The configurations used in this study are as follows; the bumpiness (B_{04}/B_{00}, where B_{04} is the bumpy component and B_{00} is the averaged magnetic field strength) are 0.15 (high), 0.06 (medium) and 0.01 (low) at the normalized radius of 0.67, respectively. The profiles of the bumpy components are shown in Fig. 2. The other field components such as the iota, the toroidicity and the helicity are kept constant among the three cases. The plasma volume, the major radius and the minor radius are also constant.

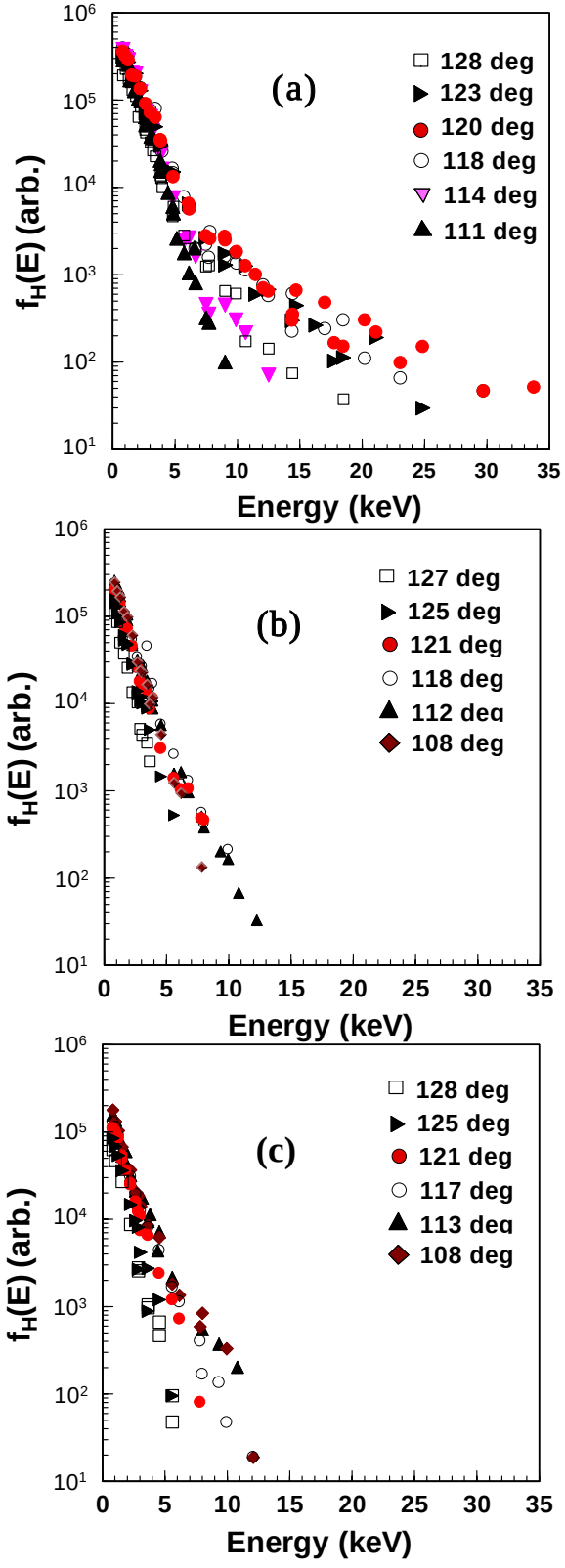

Fig. 3 Minority hydrogen spectra for various pitch angles in the high bumpy (a), the medium bumpy (b) and the low bumpy (c) configurations. By changing the toroidal and poloidal angles of the CX-NPA, the energy spectra are measured. The line of sight of the CX-NPA crosses the magnetic axis for all cases.

2. Fast Ion Confinement

High energy ions up to 30 keV were investigated by charge-exchange neutral particle analyzer (CX-NPA) for both NBI ions [7] and accelerated ions by ICRF. The former mainly includes passing particles and the latter, trapped particles. Here, the accelerated ions by ICRF are discussed. For keeping the ECH resonance position constant, the magnetic field strength is adjusted to be constant at the ECH injection position. Therefore, the magnetic field strength in the corner section where the ICRF antenna is installed is changed for each bumpy configuration, slightly. The frequency of the injected ICRF wave is adjusted so that the resonance layer is positioned near the magnetic axis: 23.2 MHz for the high bumpiness and 19 MHz for the medium and low bumpy cases. An ICRF pulse of 23.2 MHz or 19 MHz is injected into an ECH target plasma where $T_i(0)$ = 0.2 keV, $T_e(0)$ = 0.8 keV and $\overline{n}_e$ = 0.4 x 10^{19} m^{-3}. The ICRF injection power is in the range from 250 kW to 300 kW and The ECH power is about 300 kW. The minority heating mode is selected to generate fast ions with deuterium as the majority species and hydrogen as the minority species.

A CX-NPA is equipped to analyze the energetic ions, which has the ability of scanning in the toroidal and poloidal directions in order to research ions in the wide area of velocity space. It can be scanned in the toroidal direction from -10 to +18 deg and in the poloidal direction from -3 to 10 deg in order to observe charge-exchange neutrals in various pitch angles. The origin is the normal direction to the torus for the toroidal angle and the horizontal direction for the poloidal angle. The poloidal direction of the CX-NPA for measurement of each pitch angle or the field configuration is determined so that the line of sight of the CX-NPA crosses the magnetic axis.

Figure 3 shows measured minority hydrogen energy spectra for various pitch angles by changing the toroidal angle of the CX-NPA for the three bumpy cases mentioned in Section 1. In the high bumpy case (a), the ion flux is observed up to 34 keV at the pitch angle of 120 deg. Such high energy particles cannot be observed in the medium and low bumpy configurations. The highest tail is observed at about 30 deg from the perpendicular direction to the magnetic field. Toward 90 deg, the tail component decreases as shown in Fig. 3(a). The tail decreases from the angle of 120 deg as the pitch angle increases, since there is no acceleration mechanism in the parallel direction.

The high energy ion confinement is improved by increasing bumpiness. However, the measurable real space and velocity space is limited for the CX-NPA. The results of the analysis using Monte Carlo method roughly agree with the experimental results including pitch angle distribution of fast ions. The energy spectrum in the high bumpiness shows the largest high energy tail as a whole in the calculation results. The bumpiness can control the loss cone structure in this range of experiment [9].

3. Non-inductive Current

A non-inductive toroidal current plays an important role for Heliotron J since it could affect the transport through the field structure change whereas no current is required to form the confinement field. From this point of view, a non-inductive current is investigated in Heliotron J plasmas [10]. The electron cyclotron (EC) wave is injected vertically from the top port. However, the magnetic axis is not horizontal in the injection point of the EC wave. Therefore, the refractive index in the parallel direction, $n_{//}$ becomes finite. In this experiment, $n_{//}$ is 0.44. In Heliotron J plasmas, a bootstrap current, an EC driven current and a beam driven current by NBI heating are considered as the non-inductive toroidal current. Here, the BS current and the EC driven current are discussed for ECH plasmas. The BS current and the EC driven current are separated by the procedure that the EC driven current is estimated from the addition of the measured currents in the normal magnetic field and the reversed magnetic field and the BS current is from the subtraction since only the BS current changes its direction by field reversal. The BS current flows according to the field geometry and plasma parameters. The bootstrap current ($\leq$ 2 kA) flows in the co-direction in most cases as shown in Fig. 4. Here, the magnetic field strength at the axis is determined so that ω_0/ω is 0.5, where ω_0 is the cyclotron frequency at the axis and ω is the injected EC wave frequency. The current is largest in

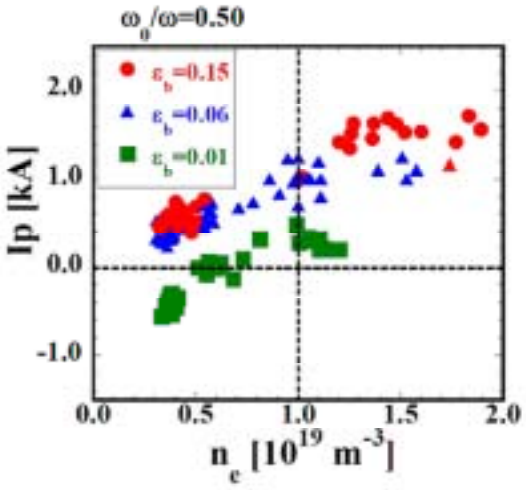

Fig. 4 Density dependence of the measured toroidal current in the three bumpy cases (in Ref. [10]). The injection condition of ω_0/ω is 0.5.

the high bumpiness and lowest in the low bumpiness. However, in the low density region for the low bumpiness,

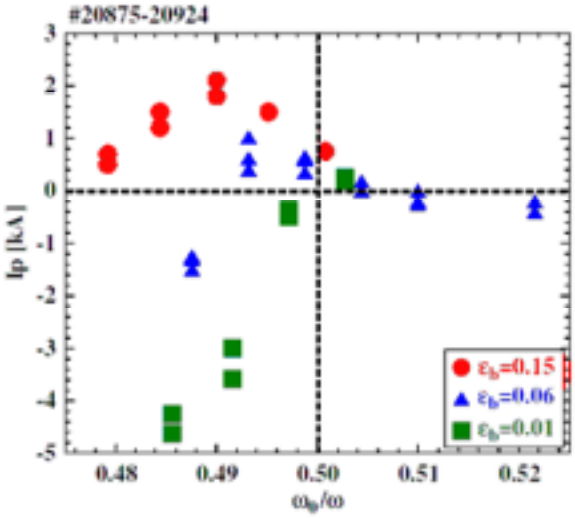

Fig. 5 The dependence of the toroidal current on the deposition position for the three bumpy cases (in Ref. [10]). The line-averaged electron density is 0.5 $\times 10^{19}$ m^{-3}.

the flow direction is reversed. The EC driven current in this condition (ω_0/ω = 0.5) is very small, then, the toroidal current is mostly a BS current in Fig. 4. The negative BS current in the low bumpy case can be explained by the neo-classical theory taking account of the possible radial electric field.

The magnitude of the EC driven current depends on the position of the EC power deposition since the effectiveness depends on the accelerated electron trajectory and its confinement. When the deposition is changed, the orbit of the energetic electron accelerated by the EC wave is considered to be changed. For example, the energetic electron in the transit orbit moves to the trapped orbit by changing acceleration position. At that time, the toroidal current component generated via Fisch-Boozer effect [11] will be changed to the opposite component generated via Ohkawa effect [12]. By changing the field strength, the toroidal current dependence on the deposition position is measured for the three bumpy cases. Near ω_0/ω = 0.49, a large toroidal current is observed for all cases as shown in Fig. 5. It is noted that the current direction can be altered by changing the bumpiness.

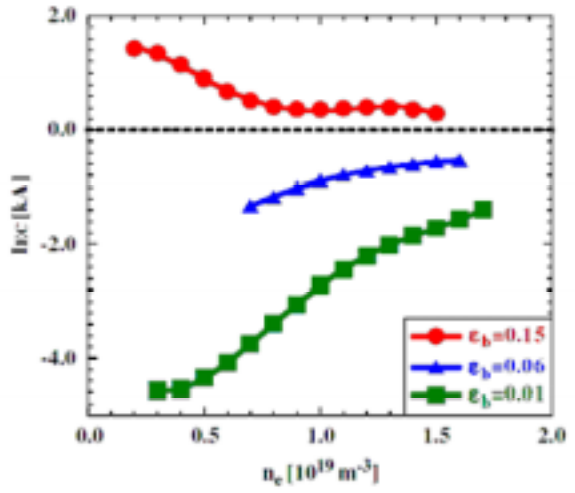

Fig. 6 Density dependence of the EC driven current at ω_0/ω = 0.49 for the three bumpy cases (in Ref. [10]).

The EC driven current at ω_0/ω = 0.49 is estimated separately as shown in Fig. 6. A positive EC driven current is generated in the high bumpiness, while a negative EC driven current is generated in the medium and the low bumpiness. The maximum EC driven current of -4.6 kA has been observed for the low bumpy configuration. The maximum current drive figure of merit is $n_e R I_p / P_{EC}$ = 8.4 × 10^{16} AW^{-1} m^{-2} (I_p = 3.2 kA, n_e = 0.7 × 10^{19} $m^{-3}$and P_{EC} = 320 kW) [10]. Here we take the injected ECH power as P_{EC}. This current drive efficiency is lower than that predicted by the linear theory. The driving mechanism for the both directions in EC current drive, which is the Fisch-Boozer effect and the Ohkawa effect, must be considered.

4. Energy Confinement

The energy confinement for ECH or NBI plasma is also studied for the three bumpy configurations. Figure 7

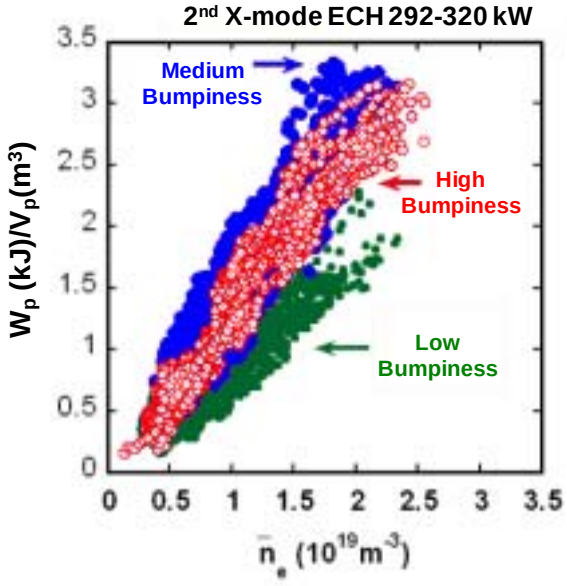

Fig. 7 Volume normalized plasma stored energy as a function of density in the three bumpy cases for ECH plasmas under the almost constant ECH power.

shows the volume normalized plasma stored energy attained as a function of density. The energy confinement is good for the medium and the high bumpy cases. The medium case is slightly better than the high bumpy case [13, 14].

For the study of NBI plasmas, one counter-injected NB unit is used since no transition phenomena to H-mode have been observed in counter injection, then the study is focused on the L-mode plasma [15, 16]. Figure 8 shows the plasma stored energy as a function of the absorbed NBI power in the three bumpy configurations for the constant density condition of 2×10^{19} m^{-3} [17]. The absorption power is estimated by using a birth-point calculation code (HFREYA), an orbit tracing code (MCNBI) and a Fokker-Planck code (FIT) [18]. The difference of the beam absorption ratio among the three

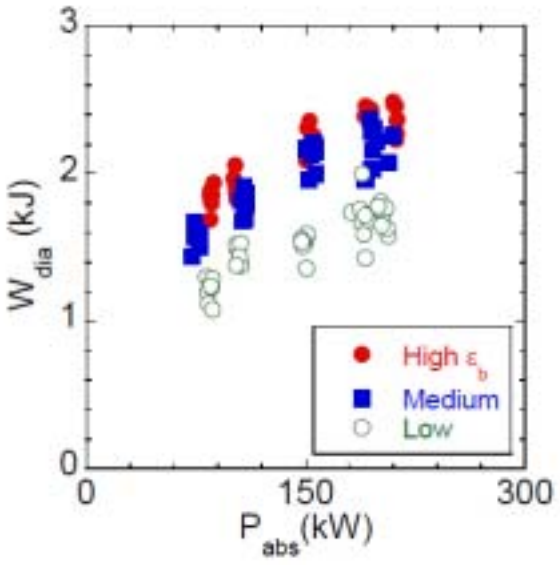

Fig. 8 Plasma stored energy as a function of absorbed NBI power for three bumpy cases. The neutral beam is injected in the counter direction under the line-averaged electron density of 2×10^{19} m^{-3}.

bumpy configurations is several percent for the density range from 1×10^{19} m^{-3} to 3×10^{19} m^{-3}. The plasma stored energy in the high and the medium bumpy cases is larger than that in the low bumpy case. The high bumpy case is best for the attained stored energy although the difference of the stored energy between the high and medium bumpy cases is not so large.

In Fig. 9, the relation between the experimental energy confinement time and the international stellarator scaling law (ISS95) is shown [17]. The beam component in the stored energy estimated from the Fokker-Planck analysis, which is less than 7%, is subtracted from the obtained stored energy. The enhancement factor of energy confinement time for the ISS95 is about 1.8, 1.7 and 1.4 in the high, the medium and the low bumpy

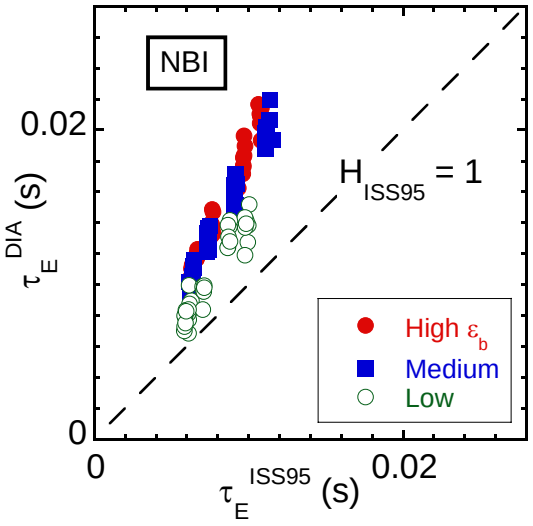

Fig. 9 The relation between the experimental energy confinement time and the international stellarator scaling law (ISS95) for the NBI plasma in the three bumpy configurations.

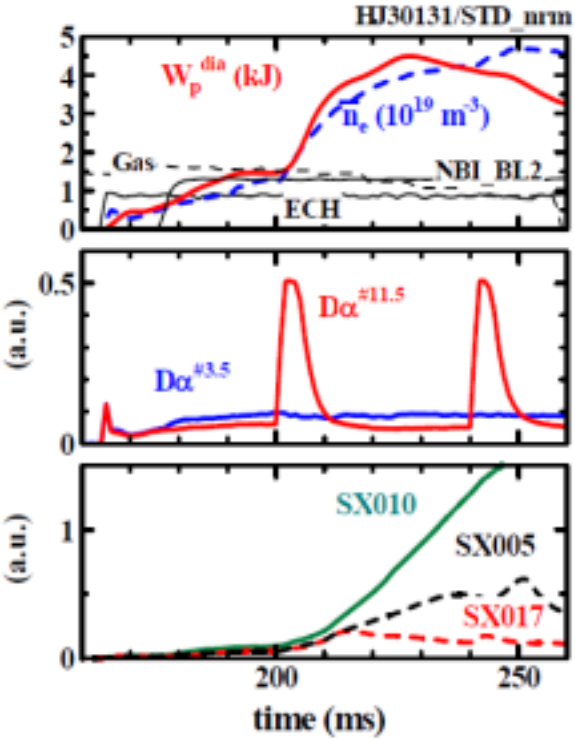

Fig. 10 The time traces of plasma parameters due to the SMBI fueling during the NBI and EC heating.

configurations, respectively. These results indicate the better confinement of the high and medium bumpy configurations. However, the medium bumpiness was most favorable for ECH plasmas in the experiment of the same density range. This difference is under investigation.

For the extension of the plasma operation region and the improvement of the confinement, the supersonic molecular beam injection (SMBI) system has been

installed [19]. This technique has been developed by L. Yao et al. [20, 21, and 22]. The SMBI fueling is performed for the plasma heated by NBI (0.6 MW) and EC wave (0.35 MW). The time traces of the line-averaged electron density ($\overline{n}_e$), the plasma stored energy (W_p), H_α, the signals of the three channels of an SX-array are shown with two pulses of SMBI in Fig. 10. After the first SMBI, the density and the stored energy are increased. The increment of the stored energy by the first pulse is large and it reaches 4.5 kJ. This value is about 50% higher than the maximum value attained by the normal gas-puff fueling for the same heating condition in Heliotron J. The plasma stored energy attained by using SMBI is extended from those by the gas-puff, which is limited at about 3 kJ for the similar EC and NBI heated plasmas. The SMBI fueling is considered to be a useful method for the optimization of the fueling for the Heliotron J plasmas.

5. Summary

The bumpy field control experiment aiming the improvement of the plasma confinement in Heliotron J has been performed.

The fast ion confinement is expected to be deeply connected to the bumpy control in Heliotron J magnetic configuration. By using ICRF minority heating, the fast ion formation and confinement is investigated in the low density condition of 0.4×10^{19} m^{-3}. The fast ion flux measured by the CX-NPA is largest in the high bumpy configuration. The flux near 30 keV is observed only in the high bumpy configuration. The high bumpy configuration is favorable for the fast-ion formation and confinement.

The non-inductive current is generated as a BS current and an EC driven current by the obliquely injected EC wave. Both the BS current and the EC driven current depend on the field configuration and plasma parameters. By changing the bumpy component, the non-inductive current at $\omega_0/\omega = 0.50$, which is mainly a BS current is changed by about 1 kA. Using the combination of the change of the bumpiness and the deposition position, the toroidal current can be controlled by about 7 kA.

For the global energy confinement, the bumpy dependence is also observed. In ECH plasmas, the medium and high bumpy configurations are better than the low bumpy configuration and the medium bumpy case is slightly better than the medium bumpy case. However, the dependence in the NBI plasmas is different from the ECH case. The high bumpy case is most favorable for the energy confinement although the difference between the high and medium cases is small. In addition to the improvement of the bulk electron confinement due to the bumpy control, it is possible that the better fast ion confinement in the high bumpy configuration improves the heating efficiency during slowing-down process of fast ions. The SMBI fueling has been performed and the stored energy of 4.5 kJ is attained. The optimization of the fueling is in progress.

Acknowledgements

This work is performed with the support and under the auspices of the Collaboration Program of the Laboratory for Complex Energy Processes, Institute of Advanced Energy, Kyoto University and the National Institute for Fusion Science (NIFS) Collaborative Research Program of NIFS04KUHL005, NIFS04KUHL002, NIFS04KUHL003, NIFS04KUHL006, NIFS06KUHL007, NIFS06KUHL009, NIFS06KUHL010, NIFS07KUHL011, NIFS07KUHL014, NIFS07KUHL015, NIFS07KUHL016, NIFS08KUHL020 and NIFS08KUHL022, the Formation of International Network for Scientific Collaborations as well as the Grant-in-Aid for Sci. Research.

References

[1] S. Gori *et al*., in Theory of Fusion Plasmas (Proc. Joint Varenna-Lausanne Int. Workshop, Varenna, 1996), Editrice Compositori, Bologna, 335 (1997).
[2] J. Nührenberg and R. Zille, Phys. Lett. A **129**, 113 (1988).
[3] J. Nührenberg *et al*., in Theory of Fusion Plasmas (Proc. Joint Varenna-Lausanne Int. Workshop, Varenna, 1994), Editrice Compositori, Bologna, 3 (1994).
[4] F. Sano *et al*., J. Plasma and Fusion Res. Series **3**, 26 (2000).
[5] M. Wakatani *et al*., Nucl. Fusion **40**, 569 (2000).
[6] T. Obiki *et al*., Nucl. Fusion **41**, 833 (2001).
[7] S. Kobayashi *et al*., IAEA-CN-116/EX/P4-41 (2004)
[8] H. Okada *et al*., Fusion Sci. Technol. **50**, 287 (2006).
[9] H. Okada *et al*., Nucl. Fusion **47**, 1346 (2007).
[10] G. Motojima *et al*., Nucl. Fusion **47**, 1045 (2007).
[11] N.J. Fisch and A.H. Boozer, Phys. Rev. Lett. **45**, 720 (1980).
[12] T. Ohkawa, General Atomics Report GA-A13837 (1976).
[13] T. Mizuuchi *et al*., Fusion Sci. Tech. **50**, 352 (2006).
[14] F. Sano *et al*., IAEA-CN-149/EX/5-5Ra (2006).
[15] S. Kobayashi *et al*., in 11th IAEA TM on H-mode Phys. Trans. Barriers (Tsukuba, 2007).
[16] T. Mizuuchi *et al*., Joint Conf. "17th Int. Toki Conf. on Phys. Flows & Turbulence in Plasmas" and "16th Int. Stellarator/Heliotron Workshop" (Toki, 2007) O-02.
[17] S. Kobayashi *et al*., in this conference.
[18] S. Murakami *et al*., Trans. Fusion Tech. **27**, 259 (1995).
[19] T. Mizuuchi *et al.,* in this conference.
[20] L. Yao, in "New Developments in Nuclear Fusion Research" (Nova Sci. Pub., 2006) pp.61-87.
[21] L. Yao *et al.*, Proc. 20th EPS Conf. on Controlled Fusion and Plasma Phys. (Lisbon, 1993) vol. **17C(I)**, p303.
[22] L. Yao *et al*., Nucl. Fusion **47**, 1399 (2007).